High-fidelity evaluation of hybrid gas-hydrate inhibition strategies

Peter J. Metaxas[1,*], Vincent W.S. Lim[1], Stuart F. McKay[2], Julie E.P. Morgan[2], Michael L. Johns[1], Zachary M. Aman[1] and Eric F. May[1]

[1]*Fluid Science and Resources, School of Engineering, University of Western Australia, 35 Stirling Highway, Perth WA 6009, Australia*

[2]*Woodside Energy Ltd., Mia Yellagonga, 11 Mount Street, Perth WA 6000, Australia* Abstract

In subsea oil and gas production, a transition away from complete gas hydrate avoidance to risk-based hydrate management has the potential to offer cost savings and improved viability for new developments. Rigorous characterization of hydrate formation probability (via the measurement of statistically significant numbers of independent hydrate formation events) represents a critical step towards accurate quantification of hydrate blockage risk. Such characterization is especially pertinent when deploying low dosage kinetic hydrate inhibitors (KHIs) which, unlike thermodynamic hydrate inhibitors (THIs), affect hydrate formation kinetics rather than thermodynamic stability envelopes. Here we demonstrate the use of a 2nd generation, Peltier-cooled, high pressure, stirred, automated lag time apparatus (HPS-ALTA) to efficiently measure hydrate formation under conditions simulating a methane dominant natural gas asset. Over 2,500 hydrate formation events were measured using a low salt content brine, enabling the production of smooth, high resolution hydrate probability distributions in the presence of three inhibitor chemical additives and combinations thereof (a corrosion inhibitor, a KHI and a conventional THI). Beyond enabling rapid, high fidelity testing of potential inhibitor interactions, the results explicitly demonstrate the ability to effectively manipulate formation probability boundaries via a

combination of thermodynamic and kinetic inhibition effects. Such hybrid inhibition strategies can be used to achieve long induction times at operationally relevant formation temperatures (over 2 days at 2.5 °C in this study) and may be more beneficial and/or cost-effective than strategies focused on complete hydrate avoidance.

*Corresponding author: peter.metaxas@uwa.edu.au

1 Introduction

Avoiding the formation of gas hydrate plugs in subsea oil and gas flowlines is critical both for safety and for ensuring production continuity [1]. Natural gas hydrates (gas-containing, ice-like clathrate solids) are thermodynamically stable at the low temperatures and high pressures typically encountered in subsea oil and gas flowlines (e.g. [2]; Figure 1). Depending on the temperature and pressure profile of a flowline, hydrate formation (and subsequent hydrate-induced plugging) can represent a genuine risk to production. However, hydrate formation will not necessarily occur immediately upon system conditions entering the hydrate stability region. This is because large scale formation can proceed only once a critically sized (stable) hydrate nucleus is formed and is able to grow [3]. The energy penalty associated with the creation of an interface between the existing fluid and the new hydrate phase makes formation both stochastic and likely to occur only at finite values of subcooling (Figure 1). Figure 1 shows a general hydrate phase equilibrium plot that illustrates how hydrate stability and formation under ramped temperatures at typical subsea conditions can be affected through the injection of various inhibitors. The subcooling, ΔT, is the difference between the system temperature and the hydrate equilibrium temperature at constant pressure and provides a measure of the driving force for hydrate formation (Figure 1).

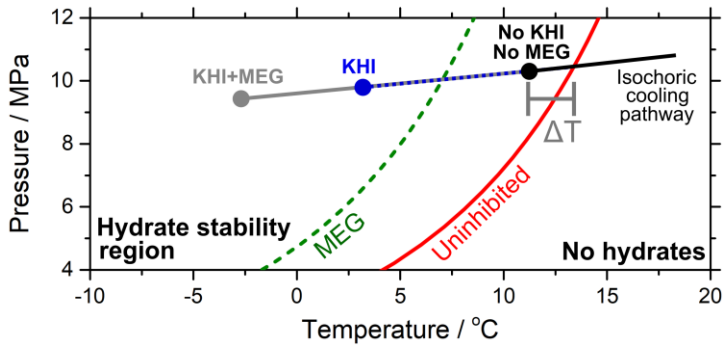

Figure 1. Calculated methane hydrate phase envelope in the absence of inhibitors and in the presence of 20 wt% MEG. Arrows show indicative isochoric cooling pathways (ramped

temperature) for uninhibited and inhibited systems with hydrate formation occurring at the filled circles (i.e. always at finite subcooling, ΔT).

Traditionally, hydrate avoidance strategies are used in subsea production systems. To achieve this, thermodynamic hydrate inhibitors (THIs), such as monoethylene glycol (MEG) or methanol, are injected into flowlines to shift the boundary of the hydrate stability region to lower temperatures, *T*, and higher pressures, *p* (see dashed curve in Figure 1). Indeed, suitable dosing of THIs can result in a subsea flowline's *p*-*T* conditions being completely outside the hydrate stability region, thereby removing any potential for hydrate formation and thus achieving complete hydrate avoidance [1]. However, THI dosage requirements for complete hydrate avoidance are typically of the order of tens of percent, making hydrate avoidance strategies costly both in terms of the THI itself and the associated infrastructure (as well as energy use) that is required for THI delivery and regeneration [4]. These costs can, in some cases, render new developments economically unviable (e.g. [5, 6]).

Unlike THIs, kinetic hydrate inhibitors (KHIs), can provide effective hydrate avoidance at dosages of a few percent. These chemicals are one of the two classes of low dosage hydrate inhibitors (LDHIs) which are used at concentrations an order of magnitude lower than that needed for THIs [5, 7, 8]; they thus have the potential to offer cost savings [8] and/or increase development viability. However, KHIs do not strongly modify the boundary of the hydrate stability region [9]. Instead, they delay the onset of hydrate formation and inhibit hydrate growth (when system conditions are within the hydrate stability region, as shown in Figure 1) (e.g. [7, 10-14]). Accurately characterizing KHI performance (e.g. in terms of how long it can delay formation onset) thus requires measurements of hydrate formation, which is a stochastic process and thus best quantified via measurements of formation probability [10-13]. Rigorous quantification of this probability as a function of system conditions requires the measurements of large numbers of

formation events, which can subsequently be used to construct representative probability distributions (typically constructed as a function of induction time and/or subcooling).

Such measurements are, however, often challenging from a time efficiency perspective since conventional systems for measuring hydrate formation can typically only have their temperatures changed slowly (e.g. [15]). This is generally due to the need to heat and cool large thermal masses (e.g. flow loops, stirred reactors or rocking cells cooled via baths or jackets). This limits the number of repeated, independent hydrate formation events which can be measured in a practical time period and thus effectively precludes the rapid collection of large formation datasets in the presence of multiple inhibitors or inhibitor combinations. In an effort to increase reproducibility, some hydrate researchers have reduced the measured degree of stochasticity in KHI-containing systems by carrying out formation experiments in the presence of what are thought to be residual hydrate structures [16-18] (formed via an initial hydrate formation event followed by incomplete dissociation). However, these approaches do not allow for the characterization of a KHI's ability to impede nucleation since hydrate structures already exist at the beginning of the measurement [11, 19]. From an industrial standpoint, these techniques also do not allow for the accurate quantification of hydrate formation likelihood from the hydrate-free fluids that enter a flowline from a wellhead at elevated temperatures [19].

Characterizing formation probability is not only critical for KHI performance testing but, more broadly, will also help inform transitions to risk-based hydrate management strategies (in contrast to hydrate avoidance). Such strategies have the potential to offer cost-savings and can improve feasibility for assets where complete hydrate avoidance is not economical (as can occur for long subsea tiebacks and/or deep-water conditions) [20-22]. When employing such strategies, a flowline may be allowed to (briefly) operate within the hydrate stability region if the associated

probability of blockage is sufficiently low. Operation within the hydrate stability region (either deliberately, or inadvertently due to, e.g., equipment failure) again requires accurate characterization of the associated hydrate formation probability. Such characterization is also important to the development of theoretical models aimed at underpinning system-wide simulations used to assess risk-based hydrate management strategies [20, 23, 24].

Formation probability needs to be quantified not only for ideal or model systems (e.g. water + methane) but also in scenarios that approach the more complex, "real-world" inhibitor environment of the flowline. Beyond hydrocarbon liquids and solids, this environment will likely include a range of inhibitors including THIs, LDHIs (KHIs and anti-agglomerants) and corrosion inhibitors (CIs). An ideal screening scenario during early production system planning would, to enable efficient system and chemical dosing optimization, include an ability to rapidly test the effect of different inhibitors, inhibitor dosages and combinations of inhibitors at various system conditions and fluid compositions (including watercut if hydrocarbon liquids are present).

Responding to the industrial requirement to quantify hydrate formation likelihood in more complex chemical scenarios, here we detail the use of the 2nd generation HPS-ALTA (high pressure, stirred, automated lag time apparatus) [13, 25] as a general tool for rapid screening of industrial hydrate inhibitor performance. The results show that this tool can be employed within practical timeframes to test the effect of varying KHI dosage, qualify the performance of what can be more economical hybrid hydrate inhibition strategies (using THIs *and* KHIs together [4, 26]) or rapidly test for interactions, favourable or unfavourable, between different inhibitors (as observed previously, for example, between KHIs and CIs [27-30]).

The HPS-ALTA consists of a series of stirred steel pressure vessels of relatively low thermal mass that can be rapidly and independently heated and cooled using thermoelectric (Peltier) elements [13, 25]. This ability to rapidly cool and heat combined with the use of pressure-based hydrate detection offers significant advantages for high fidelity measurements of hydrate formation probabilities [10, 13, 25]. It also allows the system to be taken into and out of the hydrate stability region much faster than traditional bath-cooled apparatus, yielding an overall increase in measurement rate. For example, when carrying out 1 $K \cdot min^{-1}$ system cooling, each cell, running completely independently from the others, can typically measure 1 independent hydrate formation event per hour. Furthermore, the pressure based detection method, provides advantages over optical ALTA technologies (e.g. [11]). This is because pressure-based detection enables ice and hydrate formation to be distinguished, is compatible with application of mechanical shear and measurement of opaque fluid mixtures (such as those containing crude oils) and allows for the measurement of initial hydrate growth rates based on rates of gas consumption during hydrate growth [10, 25]. Initially used primarily for measuring hydrate nucleation rates (inferred from formation onset) and testing theoretical models for hydrate formation based on hydrate-specific classical nucleation theory [3, 31], the system has recently been employed to look at the KHI-loading dependence of subcooling distributions [13]. Consistent with other studies, that work demonstrated that KHI effectiveness was reduced (per unit concentration) at high loadings. Among other demonstrations, we show here the ability to balance this performance reduction through the use of low quantities of THI, which enables additional control over hydrate formation likelihood at the (absolute) temperatures typically encountered in subsea production.

2 Experimental Section

The 2nd generation HPS-ALTA cells used in this experiment (Figure 2) have been described previously [13, 25]. Each cell has a hexagonal external cross-section and an internal cylindrical well with radius 1.2 cm and depth 2.4 cm. This corresponds to a total cell volume of 10.9 mL. Cell cooling is achieved using thermoelectric Peltier elements located on the outer edges of each cell. The cell temperature is monitored within the walls of each cell using a Pt100 resistance temperature detector (RTD) with the cell pressure measured using individual pressure transducers located between the cell and an isolation valve. During measurements, the liquid in each cell was stirred at 700 rpm using a cross-shaped, PTFE-encapsulated, magnetic flea which was driven via a magnetic stirrer located beneath the cell. All cells were housed in an air bath (i500, Steridium) maintained at approximately 32 ºC.

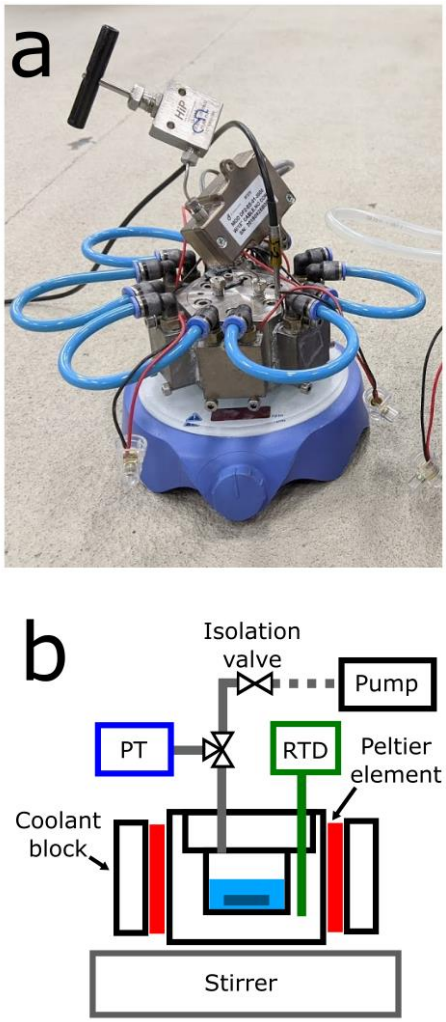

Figure 2. (a) Photo of a HPS-ALTA cell on a magnetic stirrer. (b) Simplified side-view schematic of the cell and stirrer. A syringe pump ("Pump") is connected to the cell via an isolation valve during system initialization.

Formation probability distributions for methane hydrates were primarily measured for five liquid phase compositions using two to four HPS-ALTA cells for each liquid composition. Baseline measurement tests were carried out for an aqueous 3.5 wt% NaCl solution (brine). Four other sets of measurements were carried out by adding additional inhibitors to the brine with the following quoted fractions being relative to the mass or volume of the final, inhibitor-loaded, liquid mixture: (i) 1 wt% KHI, (ii) 2 wt% KHI, (iii) 1 wt% KHI and 5 wt% MEG, and, (iv) 2 wt% KHI and 0.005

vol% CI. Both the CI and KHI are commercially available additives. To prepare the solutions, deionized water was degassed under vacuum for at least 30 minutes before adding the NaCl (and, where appropriate, additional additive(s)). In each experimental run, 5 mL of the final solution was loaded into each cell with the remainder of the cell (5.1 mL, taking into account the 0.8 cm^3 stirrer volume) filled with methane at a set initialization temperature and pressure (11 MPa and 20 °C). During initialization, the fluid was stirred at 700 RPM to ensure gas dissolution prior to sealing/isolation (after which each cell was operated isochorically).

Measurements began by first heating each cell to 40 ºC. For constant cooling measurements, the cells were then repeatedly cooled and heated to take the system conditions into and out of the hydrate equilibrium region. Following each 1 K/min^{-1} cooling ramp, the system was reheated to 40 ºC where it remained for 5 minutes to ensure dissociation of the hydrates formed during the preceding ramp. Hydrate formation was detected by post-processing the pressure and temperature data that was measured continuously during the experiment at a sampling rate of 1 Hz. Example *p-T* data obtained during a cooling ramp are shown in Figure 3.

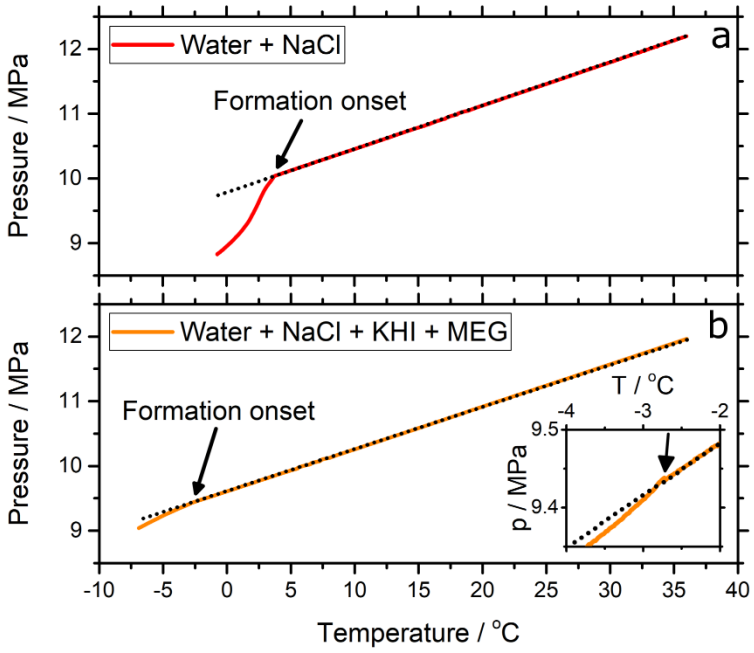

Figure 3. Cell pressure versus temperature as measured during a constant cooling ramp for the baseline system (a, red line) and in the presence of 1wt% KHI and 5 wt% MEG (b, orange line). The black dotted lines show the isochoric cooling trends prior to hydrate formation onset (black arrows). Inset in (b) shows the pressure versus temperature data in the vicinity of the formation onset event.

The onset of hydrate formation was inferred from the start of a monotonically growing reduction in the gas phase pressure relative to the isochoric pathway. The identification of the onset of this pressure reduction (at a formation pressure of p_f and a formation temperature of T_f) was carried out using an automated analysis algorithm which has been described elsewhere [10]. The small proportion of formation events occurring at the end of the linear cooling ramp or after it ((2-6) %) were not included in the datasets. For each formation event, the subcooling at which it occurred was determined by calculating the difference between the formation temperature and the dissociation temperature at the formation pressure. The latter was extracted from methane hydrate dissociation curves calculated using the Cubic-Plus-Association (CPA) model as implemented in

Multiflash ("CPA+Electrolytes") [32]. The presence of NaCl and, where appropriate, MEG, was accounted for in the subcooling calculations.

Results obtained at constant temperature in the absence of NaCl will also be presented. These latter experiments allow for a measurement of induction time and proceeded as described above except that the system was cooled to a target temperature and then remained at that value until hydrate formation was detected, again via a growth-induced pressure reduction.

3 Results and Discussion

We first consider results from experiments run under constant cooling conditions which consist of over 2,500 individual observations of hydrate formation onset. Figure 4 shows the distribution of subcooling values at formation for the baseline system (water + NaCl + methane; panel a) together with equivalent distributions obtained with the KHI dosed at (1 and 2) wt% (panels b and c). The subcooling values seen in the baseline system compare well to that detailed recently by Lim et al. [13] for methane hydrate formation from deionized water (also carried out with multiple cells). This agreement suggests a negligible measurable influence from the NaCl on formation onset kinetics (consistent with that seen for THF hydrates at a similar NaCl loading [33]). Consistent with previous studies [10, 13], in the presence of the KHI, we identify both a narrowing of the subcooling distribution and a shift to higher mean subcooling at formation onset: hydrates form at lower temperatures and thus at conditions that are further within the hydrate equilibrium region in *p*-*T* plane. The subcooling distribution obtained for 2 wt% KHI is bimodal due to differences in the base-line nucleation rates of separate cells that become resolvable with the reduced stochasticity caused by the KHIs (a similar bimodality was also observed by Lim et al. [13]).

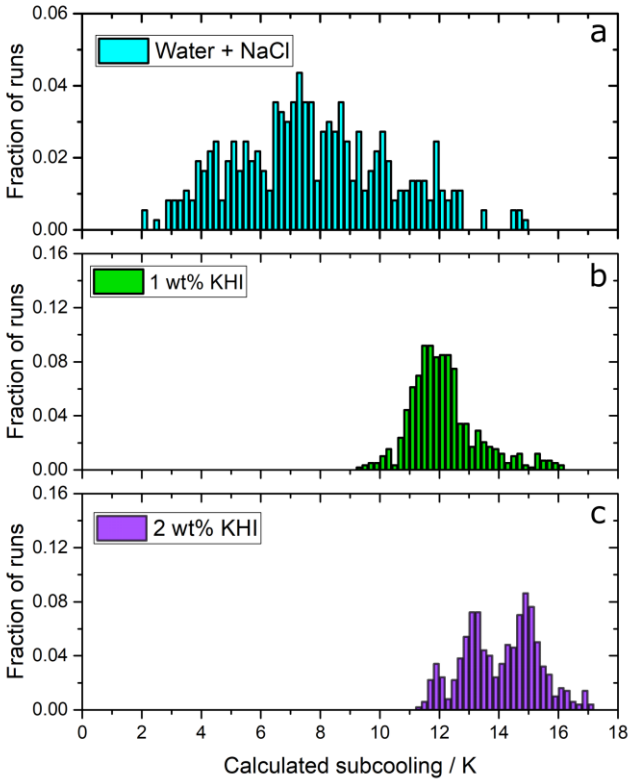

Figure 4. Subcooling probability distributions for (a) the baseline system (water + 3.5 wt% NaCl), and the baseline system with (b) 1 wt% KHI and (c) 2 wt% KHI.

The data in Figure 4 reveal that diminishing returns are obtained in terms of subcooling enhancement when the KHI loading is increased from 1 wt% to 2 wt%. Relative to the KHI-free base system, the mean subcooling increases by 4.4 K for a 1 wt% loading but only increases by another 1.9 K when the loading is doubled to 2 wt%. Analogous results in terms of diminishing returns (per unit increase in loading) have been observed both in induction time [14] and constant cooling [13] measurements, previously. For example, Lim et al. [13] found that the addition of 1 wt% KHI led to a 6.6 K increase in the mean subcooling while subsequent increases of the KHI loading to 2 wt% and 3 wt% yielded increases of only 1.1 K and 1.3 K. These values are comparable to the change in mean subcooling found here when increasing the loading from 1 wt% to 2 wt%. Below we show how the addition of a (lower cost) thermodynamic inhibitor, MEG, to

the already kinetically inhibited system can allow further reductions in the absolute formation temperatures, which is the operational quantity of primary importance. For these measurements, we limited the MEG loading to 5 wt% to ensure that the formation onset temperatures largely remained within the standard operating range of the apparatus (minimum temperature of -7 °C in the configuration used for this work).

Figure 5a shows a histogram of the formation temperatures for hydrate formation onset in the presence of 1 wt% KHI. The large subcooling values measured for this fluid composition (Figure 4b) result in hydrate formation predominantly occurring below the ice point, the average formation temperature being -1.1 °C for these ramped experiments. Adding 5 wt% MEG to the already kinetically inhibited system leads to a further decrease in the formation temperatures (red histogram in Figure 5a), decreasing the mean value to -3.0 °C and resulting in comparable formation temperatures to those obtained with 2 wt% KHI (Figure 5b): our measurements yield agreement of 0.1 K in the mean and standard deviation of the formation temperatures for the two systems. Replotting the 1 wt% KHI and 1 wt% KHI + 5 wt% MEG datasets as a function of calculated subcooling results in an overlap of the two distributions (Figure 5c), suggesting that the primary source of the shift between the distributions in Figure 5a is due to a MEG-induced thermodynamic inhibition that augments the kinetic inhibition. The addition of MEG does not significantly change the shape of the subcooling distribution (relative to the purely kinetically inhibited system) and also results in comparable mean subcooling at formation: the values differ by only 0.5 K which is within the expected uncertainty of the phase boundary calculation [34]. Figure 5d shows the formation conditions for 1 wt% KHI and 1 wt% KHI + 5 wt% MEG on a pressure-temperature plot together with the calculated dissociation curves in the absence and presence of MEG. The longer tail of the distribution for 1 wt% KHI (visible in Figure 5c at around

10 K subcooling) results in the slightly wider spread of formation conditions visible in Figure 5d when plotting each formation event as a single data-point.

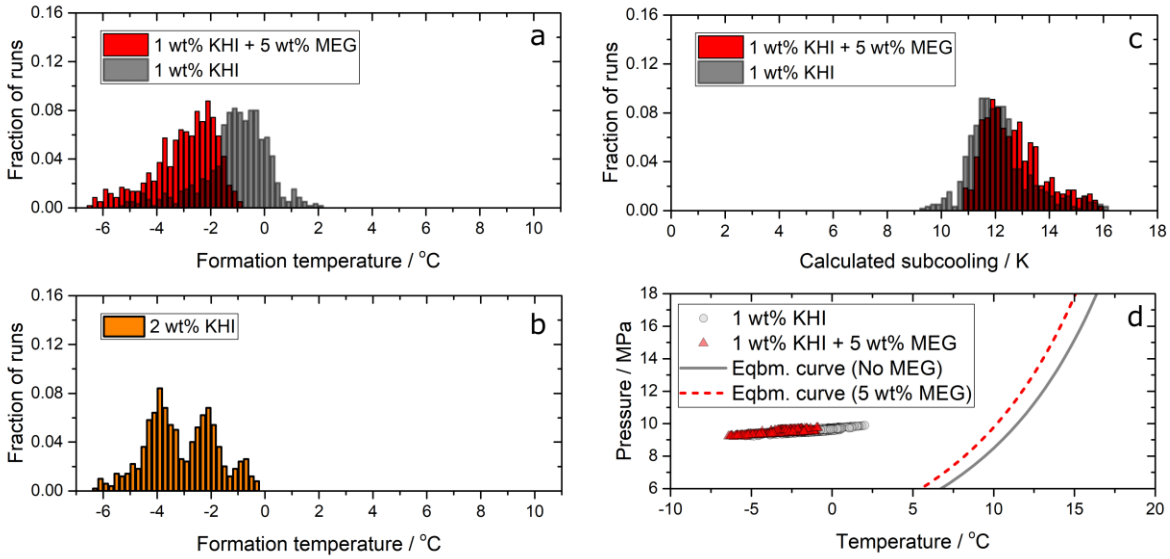

Figure 5. Formation-temperature distributions for (a) 1 wt% KHI and 1 wt% KHI + 5 wt% MEG and (b) 2 wt% KHI. (c) Calculated subcooling distibrutions for 1 wt% KHI and 1 wt% KHI + 5 wt% MEG. (d) Pressure-temperature conditions for each of the formation events used to construct (a,c), plotted together with the calculated dissociation (eqbm) curves.

In Figure 6a and b we show the mean subcoolings and mean formation temperatures, respectively, for each tested fluid. The figures highlight the diminished effect of doubling the KHI concentration from 1 wt% to 2 wt%. The data in panel b again demonstrate the comparable performance obtained for 2 wt% KHI and 1 wt% KHI with 5 wt% MEG. The results obtained from experiments that were run to confirm the absence of any detrimental effects from the addition of a film forming corrosion inhibitor to the 2wt% KHI system are also shown: the mean formation temperature (and calculated subcooling) were comparable for these two mixtures.

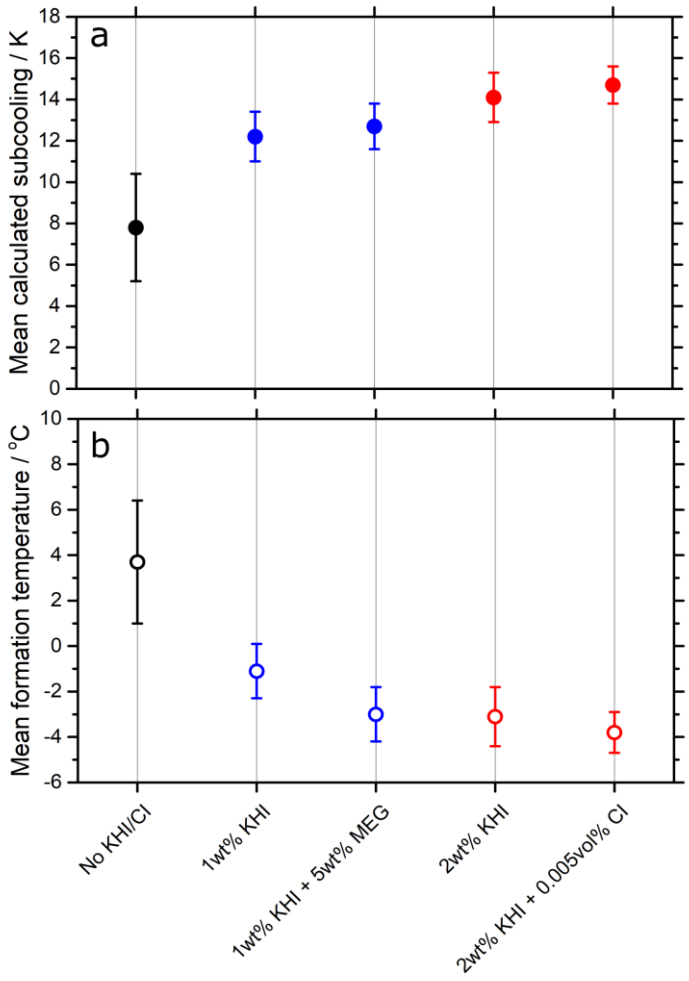

Figure 6. (a) Mean calculated subcooling and (b) mean formation onset temperature for each fluid. The error bars indicate the standard deviations for each dataset.

With one cooling-heating cycle taking approximately 1 hour, the ramped experiments run with the HPS-ALTA facilitate meaningful comparisons of formation temperatures for differing inhibitors and inhibitor mixtures. Thus the technique offers a high resolution method for inhibitor screening that is especially time-efficient for comparisons across multiple fluids, inhibitor chemistries, and/or concentrations. Consistent with the thermally activated nature of hydrate nucleation however, the obtained distributions will be cooling rate dependent. This will result in formation occurring at lower subcoolings for slower temperature ramping [35-37]. As such, ramping rates

need to be held constant across a set of experiments to enable meaningful comparison between differing inhibitor chemistries. It is however possible in principle to extract parameters from constant cooling measurements that can be used to predict subcooling-dependent mean induction times [10] which can then be directly compared to pipeline residence times. However, care must be taken to avoid artefacts associated with the dynamic nature of scanning experiments from corrupting the experiments [38]. Accordingly, it can be helpful to conduct tests that, while less time efficient, provide confirmation of the qualitative change in hydrate formation probability produced by a particular inhibition strategy at a given operating condition.

To this end, we conclude by presenting a comparison of the change in induction time at (2.5 °C, 10.3 MPa) achieved when a methane + water system containing both a THI and KHI (2 wt%) has its THI concentration doubled (10 wt% MEG to 20 wt%). The induction time considered here is defined as the time between reaching the target temperature and detecting formation onset. The HPS-ALTA's rapid cooling capability (3 $K.min^{-1}$ in these tests) means that a fixed subcooling condition can be quickly reached and ensures that the period spent within the hydrate stability region at temperatures above the target subcooling (approximately 3 minutes) is minimized (Figure 7a). The time spent at variable subcooling is 2 to 3 orders of magnitude shorter than the mean induction time measured at the constant target temperature, which means the impact of the ramp on the results obtained is negligible.

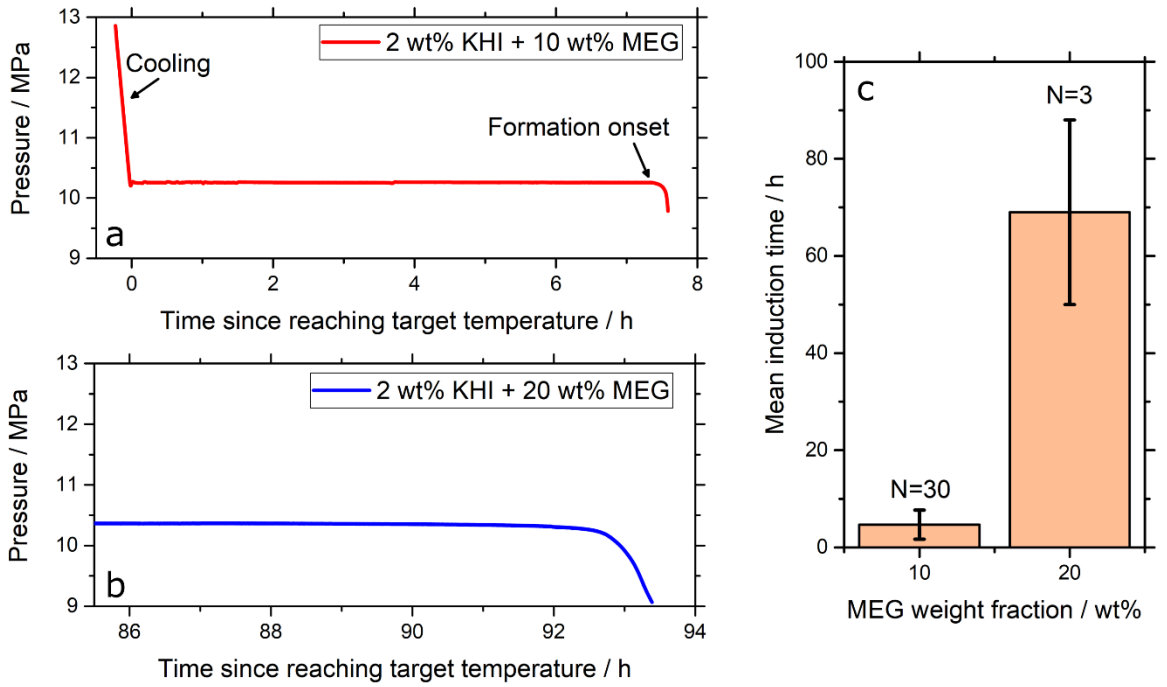

Figure 7. (a and b) Induction time measurements with 2 wt% KHI + (10 or 20) wt% MEG at 2.5 °C and 10.3 MPa which corresponds to a subcooling of approximately 10.8 K relative to the calculated dissociation curve in the *absence* of MEG. (c) Mean induction times for the N experiments carried out for the two MEG weight fractions. Error bars are standard deviations.

Increasing the MEG loading from (10 to 20) wt% changes the calculated subcooling at (2.5 °C, 10.3 MPa) from (8.2 to 4.8) K (complete hydrate avoidance at these conditions would require a MEG loading exceeding 30 wt%). With KHI dosed at 2 wt %, the result of the reduced driving force on the observed induction times is dramatic, as shown in Figure 7c. In the presence of the KHI, approximately halving the driving force increases the average induction time by an order of magnitude from (4.7±3.0) h (30 independent measurements) to (69±19) h (3 independent measurements). While the theoretical relationship between subcooling and induction times has been discussed previously (e.g. [3, 12, 25]) this test shows the practical consequence with respect to a fixed absolute temperature, constrained by operational conditions. Moreover, the reduced driving force has the additional effect of reducing the hydrate growth-rate observed following the

much-delayed formation (compare Figure 7a and b) [13, 25, 39, 40], a result which is also of importance when developing hydrate risk-management strategies.

4 Conclusion

We have demonstrated the use of a 2nd generation HPS-ALTA for rapid testing of hydrate inhibition for sheared fluids in the presence of thermodynamic hydrate inhibitors, a commercial kinetic hydrate inhibitor and a commercial corrosion inhibitor. Rapid constant cooling measurements (approximately 1 data point per hour per cell) enabled the construction of high-resolution subcooling distributions and, subsequently, a high-fidelity comparison between the impacts of varying inhibitor chemistries on hydrate formation.

Some of the most industrially pertinent outcomes relate to the results obtained using hybrid KHI+THI inhibition. Adding 5 wt% MEG to the 1 wt% KHI system led to a 1.9 K reduction in the mean formation temperature that could be largely explained via the calculated change in the subcooling due to MEG-induced thermodynamic inhibition. Comparable mean formation onset temperatures were achieved either for 2 wt% KHI or (1 wt% KHI + 5 wt% MEG). These results not only confirm the absence of any major antagonistic effects when using this hybrid inhibition strategy, but also highlight the ability to manipulate formation probability boundaries using combinations of thermodynamic and kinetic inhibitors. This can be useful given the diminishing returns in terms of inhibition performance (per dosing unit) that can be associated with increased KHI dosage.

Induction time measurements involving fast cooling (3 $K.min^{-1}$) to a target measurement temperature were also employed to confirm qualitatively the improved inhibition performance achieved with hybrid strategies, particularly with respect to (e.g.) pipeline residence times. Unlike

conventional apparatus, the HPS-ALTA enables a temperature of interest (or given subcooling) to be obtained in a matter of minutes and then remain there until hydrates form. This ability greatly reduces the influence of the cooling ramp (during which the subcooling is constantly changing) on the measured formation kinetics, even when induction times are of the order 1000 s or less. An order of magnitude increase in mean induction time (approximately (5 to 70) h) was observed at a fixed temperature and pressure by increasing the MEG weight fraction from 10 wt% to 20 wt% in the presence of 2 wt% KHI. This was achieved at (2.5 °C, 10 MPa) which corresponds to a subcooling in excess of 10 K relative to the calculated dissociation conditions in the absence of any inhibitors.

Acknowledgements

This work was funded by Woodside Energy Ltd and the Australian Research Council through FT180100572 and also IC150100019 as part of the ARC Industrial Transformation and Training Centre for LNG Futures.

References

1. Sloan, E.D., et al., *Natural Gas Hydrates in Flow Assurance.* Natural Gas Hydrates in Flow Assurance, 2011: p. 1-200.
2. Cochrane, S. *Hydrate Control and Remediation Best Practices in Deepwater Oil Environments*. in *Offshore Technology Conference*. 2003. Houston, Texas, USA.
3. Kashchiev, D. and A. Firoozabadi, *Nucleation of gas hydrates.* Journal of Crystal Growth, 2002. **243**(3-4): p. 476-489.
4. Szymczak, S., et al., *Chemical Compromise: A Thermodynamic and Low-Dose Hydrate-Inhibitor Solution for Hydrate Control in the Gulf of Mexico.* SPE Projects, Facilities & Construction, 2006. **1**(04): p. 1-5.

5. Glenat, P., et al., *South-Pars Phases 2 and 3: The Kinetic Hydrate Inhibitor (KHI) Experience Applied at Field Start-up*, in *Abu Dhabi International Conference and Exhibition*. 2004, Society of Petroleum Engineers: Abu Dhabi, United Arab Emirates. p. 6.
6. Phillips, N.J. and M. Grainger, *Development and Application of Kinetic Hydrate Inhibitors in the North Sea*, in *SPE Gas Technology Symposium*. 1998, Society of Petroleum Engineers: Calgary, Alberta, Canada. p. 8.
7. Kelland, M.A., *History of the Development of Low Dosage Hydrate Inhibitors.* Energy & Fuels, 2006. **20**(3): p. 825-847.
8. Kelland, M.A., *Production Chemicals for the Oil and Gas Industry, Second Edition*. 2nd ed. ed. 2014, Boca Raton: CRC Press.
9. Tohidi, B., et al., *Improving the accuracy of gas hydrate dissociation point measurements.* Gas Hydrates: Challenges for the Future, 2000. **912**: p. 924-931.
10. May, E.F., et al., *Gas Hydrate Formation Probability Distributions: The effect of shear & comparisons with nucleation theory.* Langmuir, 2018. **34**: p. 3186.
11. May, E.F., et al., *Quantitative kinetic inhibitor comparisons and memory effect measurements from hydrate formation probability distributions.* Chemical Engineering Science, 2014. **107**: p. 1-12.
12. Ke, W., et al., *Inhibition-Promotion: Dual Effects of Polyvinylpyrrolidone (PVP) on Structure-II Hydrate Nucleation.* Energy & Fuels, 2016. **30**(9): p. 7646-7655.
13. Lim, V.W.S., et al., *Gas hydrate formation probability and growth rate as a function of kinetic hydrate inhibitor (KHI) concentration.* Chemical Engineering Journal, 2020. **388**: p. 124177.
14. Kang, S.-P., et al., *Experimental measurement of the induction time of natural gas Hydrate and its prediction with polymeric kinetic inhibitor.* Chemical Engineering Science, 2014. **116**: p. 817-823.
15. Abay, H.K. and T.M. Svartaas, *Multicomponent Gas Hydrate Nucleation: The Effect of the Cooling Rate and Composition.* Energy & Fuels, 2011. **25**(1): p. 42-51.
16. Peytavy, J.L., P. Glenat, and P. Bourg. *Qualification of Low Dose Hydrate Inhibitors (LDHIs): Field Cases Studies Demonstrate the Good Reproducibility of the Results Obtained from Flow Loops*. in *6th International Conference on Gas Hydrates (ICGH 2008)*. 2008. Vancouver, British Columbia, Canada.

17. Duchateau, C., et al., *Laboratory Evaluation of Kinetic Hydrate Inhibitors: A Procedure for Enhancing the Repeatability of Test Results.* Energy & Fuels, 2009. **23**(2): p. 962-966.
18. Mozaffar, H., R. Anderson, and B. Tohidi, *Reliable and Repeatable Evaluation of Kinetic Hydrate Inhibitors Using a Method Based on Crystal Growth Inhibition.* Energy & Fuels, 2016. **30**(12): p. 10055-10063.
19. McNamee, K. and P. Conrad. *The Effect of Autoclave Design and Test Protocol on Hydrate Test Results*. in *7th International Conference on Gas Hydrates (ICGH 2011)*. 2011. Edinburgh, Scotland, United Kingdom.
20. Norris, B.W.E., et al., *Risk-Based Flow Assurance Design for Natural Gas Hydrate Production Systems*, in *Offshore Technology Conference Asia*. 2018, Offshore Technology Conference: Kuala Lumpur, Malaysia. p. 10.
21. Creek, J.L., S. Subramanian, and D.A. Estanga, *New Method for Managing Hydrates in Deepwater Tiebacks*, in *Offshore Technology Conference*. 2011, Offshore Technology Conference: Houston, Texas, USA.
22. Sloan, E.D., *A changing hydrate paradigm - from apprehension to avoidance to risk management.* Fluid Phase Equilibria, 2005. **228**: p. 67-74.
23. Charlton, T.B., et al., *Predicting Hydrate Blockage Formation in Gas-Dominant Systems*, in *Offshore Technology Conference Asia*. 2018, Offshore Technology Conference: Kuala Lumpur, Malaysia. p. 13.
24. May, E.F., et al., *Managing Hydrate Formation in Subsea Production*, in *Offshore Technology Conference*. 2020, Offshore Technology Conference: Houston, Texas, USA. p. 13.
25. Metaxas, P.J., et al., *Gas hydrate formation probability distributions: Induction times, rates of nucleation and growth.* Fuel, 2019. **252**: p. 448-457.
26. Budd, D., et al., *Enhanced Hydrate Inhibition in Alberta Gas Field*, in *SPE Annual Technical Conference and Exhibition*. 2004, Society of Petroleum Engineers: Houston, Texas. p. 8.
27. Moloney, J.J., W.Y. Mok, and C.G. Gamble, *Compatible Corrosion And Kinetic Hydrate Inhibitors For Wet Sour Gas Transmission Lines*, in *CORROSION 2009*. 2009, NACE International: Atlanta, Georgia. p. 23.

28. Woie, K., *A study of the interaction between a kinetic hydrate inhibitor and selected corrosion inhibitors*. 2011, University of Stavanger.
29. Jones, R., et al., *Development of a Novel Kinetic Hydrate Inhibitor and Corrosion Inhibitor Package for Wet Gas Application*, in *OTC Brasil*. 2013, Offshore Technology Conference: Rio de Janeiro, Brazil. p. 14.
30. Moore, J., L.V. Vers, and P. Conrad, *Understanding Kinetic Hydrate Inhibitor and Corrosion Inhibitor Interactions*, in *Offshore Technology Conference*. 2009, Offshore Technology Conference: Houston, Texas. p. 20.
31. Kashchiev, D. and A. Firoozabadi, *Induction time in crystallization of gas hydrates.* Journal of Crystal Growth, 2003. **250**(3-4): p. 499-515.
32. *MultiFlash 6.2*. 2016, Infochem/KBC Advanced Technologies plc.
33. Sowa, B., et al., *Formation of Ice, Tetrahydrofuran Hydrate, and Methane/Propane Mixed Gas Hydrates in Strong Monovalent Salt Solutions.* Energy & Fuels, 2014. **28**(11): p. 6877-6888.
34. Ballard, L. and E.D. Sloan, *The next generation of hydrate prediction IV: A comparison of available hydrate prediction programs.* Fluid Phase Equilibria, 2004. **216**(2): p. 257-270.
35. Ke, W. and T.M. Svartaas. *Effects of stirring and cooling on methane hydrate formation in a high-pressure isochoric cell*. in *7th International Conference on Gas Hydrates (ICGH 2011)*. 2011. Edinburgh, Scotland, United Kingdom.
36. Maeda, N., *Nucleation curves of methane hydrate from constant cooling ramp methods.* Fuel, 2018. **223**: p. 286-293.
37. Maeda, N., *Nucleation curves of methane – propane mixed gas hydrates in hydrocarbon oil.* Chemical Engineering Science, 2016. **155**: p. 1-9.
38. Kulkarni, S.A., et al., *Crystal Nucleation Kinetics from Induction Times and Metastable Zone Widths.* Crystal Growth & Design, 2013. **13**(6): p. 2435-2440.
39. Turner, D., et al., *Development of a hydrate kinetic model and its incorporation into the OLGA2000 transient multi-phase flow simulator,* in *Fifth International Conference on Gas Hydrates*. 2005: Trondheim, Noway.
40. Vysniauskas, A. and P.R. Bishnoi, *A Kinetic-Study of Methane Hydrate Formation.* Chemical Engineering Science, 1983. **38**(7): p. 1061-1072.

TOC image

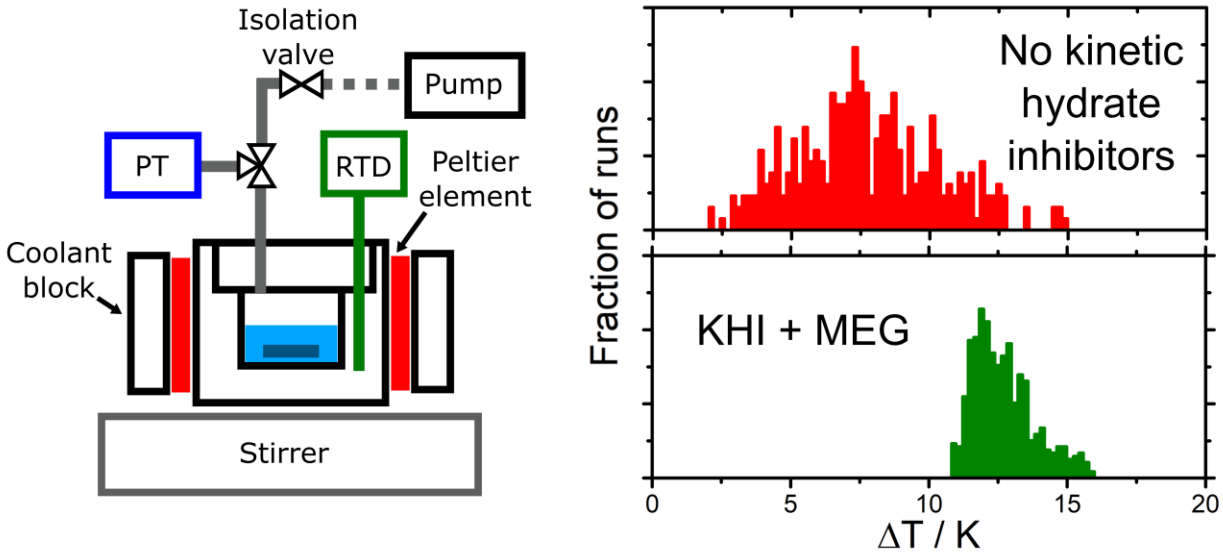
Isolation valve
Pump
PT
RTD
Peltier element
Coolant block
Stirrer
Fraction of runs
No kinetic hydrate inhibitors
KHI + MEG
0
5
10
15
20
ΔT / K